Charged particle layers in the Debye limit

Kenneth I. Golden*
Department of Mathematics and Statistics and Department of Physics, University of Vermont, Burlington, Vermont 05401-1455

Gabor J. Kalman† and Stamatios Kyrkos‡
Department of Physics, Boston College, Chestnut Hill, Massachusetts 02467
(Received 23 May 2002; published 27 September 2002)

We develop an equivalent of the Debye-Hückel weakly coupled equilibrium theory for layered classical charged particle systems composed of one single charged species. We consider the two most important configurations, the charged particle bilayer and the infinite superlattice. The approach is based on the link provided by the classical fluctuation-dissipation theorem between the random-phase approximation response functions and the Debye equilibrium pair correlation function. Layer-layer pair correlation functions, screened and polarization potentials, static structure functions, and static response functions are calculated. The importance of the perfect screening and compressibility sum rules in determining the overall behavior of the system, especially in the $r\rightarrow\infty$ limit, is emphasized. The similarities and differences between the quasi-two-dimensional bilayer and the quasi-three-dimensional superlattice are highlighted. An unexpected behavior that emerges from the analysis is that the screened potential, the correlations, and the screening charges carried by the individual layers exhibit a marked nonmonotonic dependence on the layer separation.

DOI: 10.1103/PhysRevE.66.031107 PACS number(s): 05.20.−y, 68.65.Ac, 68.65.Cd, 52.27.Gr

I. INTRODUCTION

Layered systems consisting of classical charged particles have been realized in various laboratory experiments. Examples are ionic layers in Penning traps [1,2] and layers of charged mesoscopic grains in complex (dusty) plasmas [3]. The layer formation in trapped cryogenic ions was first pointed out on theoretical grounds by Dubin [2] and subsequently verified experimentally [1(d)]. Charged particle layered systems are of importance in many other physical systems such as semiconductor nanostructures, metallic superlattices, nested nanotubes, etc. While these latter systems are not classical, since the constituent electrons are fully or partially degenerate, a classical modeling provides, in many cases, a good qualitative description. This is especially so with regard to the *interlayer correlations*, since in most cases interlayer exchange and tunneling are negligible.

While the number of lattice planes, N, in the different layer configurations can vary, the two extremes $N=2$ and $N\gg 1$, $(N\rightarrow\infty)$, have attracted the most experimental and theoretical interest. An important parameter in all scenarios is the plasma coupling parameter, representing the ratio of the Coulomb energy to kinetic energy. If the system consists of classical charged particles (ions or grains), the source of the kinetic energy is temperature and the *intralayer* coupling parameter $\Gamma=Z^2e^2/(ak_BT)$; $a=1/\sqrt{\pi n}$ is the two-dimensional (2D) Wigner-Seitz radius. However, for the weak coupling $(\Gamma<1)$ domain of interest in the present paper, the length scale is set not by the Wigner-Seitz radius, but rather by the 2D Debye wave number $\kappa=2\pi nZ^2e^2/(k_BT)$. In this domain, the coupling strength accordingly is measured by the traditional plasma parameter $\gamma=(Z^2e^2\kappa)/(k_BT)=\kappa^2/(2\pi n)=(2\pi nZ^4e^4)/(k_BT)^2<1$; note the relationship $\gamma=2\Gamma^2$. The measure of the *interlayer* coupling strength between the layers spaced a distance d apart is characterized by the coupling parameter $Z^2e^2/(dk_BT)=\Gamma(a/d)=\gamma/(\kappa d)$.

Over the past decade, substantial theoretical interest has been directed at the static properties of layered systems. For charged particle bilayers the remarkable influence of the interlayer coupling on the static response properties was first pointed out by Swierkowski *et al.* [4], followed by the Monte Carlo studies of Rapisada and Senatore [5]. The structure and phonon excitations of the bilayer crystal were analyzed by Goldoni and Peeters [6] and by Falko [7], leading to the prediction of structural phase transformations. The structural features in the strongly coupled bilayer liquid phase were subsequently examined via a classical hypernetted-chain calculation by Kalman and co-workers [8,9]. More recently, molecular dynamics studies of both electron-electron and electron-hole bilayers were done by Donko and co-workers [9,10], and Weis, Levesque, and Jorge [11].

As to superlattices, interest in the effect of interlayer interaction on the static response and screening potentials started with the early random-phase approximation (RPA) treatment of Visscher and Falicov [12] for a zero-temperature degenerate system. Going beyond the RPA, Kalman, Ren, and Golden [13] introduced an iterative scheme to generate interlayer pair correlation functions from known correlation functions of the isolated 2D system. In contrast to the bilayer, a more systematic procedure for calculating the pair correlation functions in a superlattice has yet to be worked out.

In this paper we have developed the equivalent of the Debye-Hückel (DH) weakly coupled equilibrium theory for layered classical charged particle systems composed of one single charged species. Layered ionic systems formed in

*Electronic address: golden@emba.uvm.edu
†Electronic address: kalman@bc.edu
‡Electronic address: kyrkos@bc.edu

laboratory experiments are necessarily strongly coupled and are therefore not well described by the present calculation. Semiconductor bilayers and other fully or partially degenerate systems are, on the other hand, mostly weakly coupled; here the classical DH theory would provide a qualitative (but in the absence of a proper treatment of the exchange, quantitatively unreliable) insight into their static behavior. Nevertheless, the DH calculation is of fundamental theoretical interest, for it provides the only exact solution for the correlation and structure functions in layered systems and as such illuminates the interplay of the interparticle coupling and interlayer separation. We consider the two extreme (and most easily tractable) and, at the same time, also the most important configurations: the bilayer and the infinite superlattice. As much as it is possible, we attempt to parallel the treatments for these two systems, emphasizing both the similarities and differences.

Our model is devoid of all the possible complexities that arise from an asymmetry between the layers. We assume that all charges, masses, densities, and layer separations are identical. The quantities of interest that we focus on are the static density response function $\chi(\mathbf{k})$, the related static dielectric function $\varepsilon(\mathbf{k})$, and, most notably, the static structure function $S(\mathbf{k})$; $\mathbf{k}$ is the in-plane wave vector. In the case of the bilayer, these quantities are in fact matrices in the two-dimensional layer space; for the superlattice, they are either infinite-dimensional matrices or, more commonly, depend on the additional wave vector q, portraying the periodic variation along the superlattice axis.

The DH expressions for the $S_{11}(\mathbf{k})$, $S_{12}(\mathbf{k})$ elements of the bilayer structure function matrix and their superlattice counterparts $S_{00}(\mathbf{k})$, $S_{01}(\mathbf{k})$ have already been reported in a preliminary study by the authors and Ren [14]. In the present paper, we elaborate on the derivation of these matrix elements and then go much further in several respects. It is not our purpose to give a detailed account of the physical information that can be gleaned from the structure functions [8,9], but rather to demonstrate the overall behavior of the bilayer and superlattice structure functions and their companion pair correlation functions, in particular their differences and similarities. This can, to some extent, be accomplished via the compressibility sum rules [9,15–17], but a more explicit display can be provided by the Debye calculation of the present paper.

Additional quantities of interest are the polarization potential $[\overline{\Phi}_i(\mathbf{r};d)]$ and the (total) screened potential $[\Phi_i(\mathbf{r};d)]$ in the different layers generated as a response to the presence of a charged impurity placed in one of the layers. One of the convenient concomitants of the Debye approximation is that these potentials are directly related to the pair correlation functions $h_{ij}(\mathbf{r})$ on the one hand, and to the total correlation energy of the system on the other.

The plan of the paper is as follows. Sections II and III discuss bilayers and superlattices, respectively. For both configurations, we derive the DH expressions for the intralayer and interlayer structure functions $[S_{ij}(\mathbf{k};d)]$ and we generate the corresponding equilibrium pair correlation functions $[h_{ij}(\mathbf{r};d)]$ and accompanying screened and polarization potentials. We discuss their remarkable nonmonotonic dependence on the interlayer separation distance d that prevails in both configurations. We invoke compressibility sum rules for bilayers [9,15–17] and superlattices [16,17]. With the aid of these sum rules, we analyze the long-wavelength ($k\to 0$) limit of $S_{ij}(\mathbf{k})$ and the corresponding asymptotic ($r\to\infty$) behavior of $h_{ij}(\mathbf{r})$. Formally, the compressibility rules exhibit quite different structures for bilayers and superlattices and as a result the asymptotic ($r\to\infty$) behavior of the pair correlation functions for the two configurations is fundamentally different. From the physical point of view, these different behaviors can be understood by contrasting the quasi-two-dimensionality of the bilayer with the quasi-three-dimensionality of the superlattice. Conclusions are drawn in Sec. IV where the similarities and substantial physical differences between the bilayer and superlattice are discussed.

II. CHARGED PARTICLE BILAYERS

A. Response functions

We consider a bilayer model, consisting of two 2D layers of charged particles (with $Z=1$) of equal areal densities n, separated by a distance d. Each layer is immersed in a neutralizing background of opposite charge. The charged particles obey classical statistics. The bilayer is isomorphic to a two-component plasma and its interaction matrix elements are $\phi_{11}(k)=\phi_{22}(k)=2\pi e^2/k$, $\phi_{12}(k)=\phi_{21}(k)=(2\pi e^2/k)\exp(-kd)$. With the aid of $\phi_{ij}(k)$ and $\overline{\chi}_{ij}(\mathbf{r})$, the screened (total) density response function, the dielectric matrix $\varepsilon_{ij}(\mathbf{k})$, its inverse $\eta_{ij}(\mathbf{k})$, and the full (external) density response $\chi_{ij}(\mathbf{k})$ can be constructed,

$$\varepsilon_{ij}(\mathbf{k})=\delta_{ij}-\phi_{il}(k)\overline{\chi}_{lj}(\mathbf{k}), \tag{1}$$

$$\chi_{ij}(\mathbf{k})=\overline{\chi}_{il}(\mathbf{k})\,\eta_{lj}(\mathbf{k}), \tag{2}$$

$$\eta_{ij}(\mathbf{k})=\delta_{ij}+\phi_{il}(k)\chi_{lj}(\mathbf{k}). \tag{3}$$

Summation over repeated indices is understood.

Our purpose in this paper is to calculate the structure and pair correlation functions to lowest order in the coupling parameter γ. This is clearly equivalent to the customary DH approximation. To this order the fluctuation-dissipation relations link the $S_{ij}(\mathbf{k})$ matrix elements to the Vlasov (RPA) $\chi_{ij}(\mathbf{k})$ matrix elements. In turn, in the Vlasov approximation the screened response function $\overline{\chi}_{ij}(\mathbf{k})$ is identical to the response function of the noninteracting gas and is necessarily diagonal [18]. This feature can be adopted as the starting point for the calculation,

$$\overline{\chi}_{ij}(\mathbf{k})=-\beta n\,\delta_{ij}, \tag{4}$$

$\beta\equiv 1/(k_BT)$. The full density response matrix is then calculated from Eqs. (2) and (4),

$$\chi_{ij}(\mathbf{k})=-\beta n\,\eta_{ij}(\mathbf{k}), \tag{5}$$

whence from Eqs. (5) and (3),

$$\eta_{11}(\mathbf{k})=\eta_{22}(\mathbf{k})=\frac{\tilde{k}(1+\tilde{k})}{(1+\tilde{k})^2-\exp(-2\tilde{k}\tilde{d})}, \tag{6a}$$

$$\eta_{12}(\mathbf{k})=\eta_{21}(\mathbf{k})=-\frac{\tilde{k}\exp(-\tilde{k}\tilde{d})}{(1+\tilde{k})^2-\exp(-2\tilde{k}\tilde{d})}, \tag{6b}$$

($\tilde{k}\equiv k/\kappa, \tilde{d}\equiv\kappa d$). The matrix elements

$$\eta_{11}(k=0)-1=-\frac{1}{2}\left(\frac{1+2\tilde{d}}{1+\tilde{d}}\right), \tag{7a}$$

$$\eta_{12}(k=0)=-\frac{1}{2(1+\tilde{d})} \tag{7b}$$

represent the total screening charges residing in layers 1 and 2, respectively, surrounding a $Z=+1$ impurity charge in layer 1. Expressions (7a) and (7b) exhibit the expected monotonic dependence on the layer separation d (to be contrasted with the corresponding nonmonotonic expression (36) for the superlattice).

B. Structure functions

Invoking the classical fluctuation-dissipation theorem (FDT)

$$S_{ij}(\mathbf{k})=-\frac{1}{\beta n}\chi_{ij}(\mathbf{k}) \tag{8}$$

and the RPA full density response (5), one readily obtains

$$S_{ij}(\mathbf{k})=\eta_{ij}(\mathbf{k}). \tag{9}$$

At long wavelengths, Eqs. (9), (6a) and (6b) reproduce the RPA limit of the expressions

$$S_{11}(k\to 0)=\frac{1}{2}\frac{1}{L-N+\tilde{d}}+\frac{1}{4}\left[1+\frac{\tilde{d}^2}{(L-N+\tilde{d})^2}\right]\tilde{k}+O(\tilde{k}^2), \tag{10a}$$

$$S_{12}(k\to 0)=-\frac{1}{2}\frac{1}{L-N+\tilde{d}}+\frac{1}{4}\left[1-\frac{\tilde{d}^2}{(L-N+\tilde{d})^2}\right]\tilde{k}+O(\tilde{k}^2), \tag{10b}$$

derived from the compressibility sum rules [9,15–17]. In this limit, the direct inverse compressibility $L\equiv L_{11}\equiv\beta(\partial P_1/\partial n_1)=\beta(\partial P_2/\partial n_2)\equiv L_{22}$ equals unity and the trans-inverse compressibility $N\equiv L_{12}\equiv\beta(\partial P_1/\partial n_2)=\beta(\partial P_2/\partial n_1)\equiv L_{21}$ equals zero. In deriving Eqs. (10a) and (10b), it should be emphasized that the expansion of $\exp(-kd)$ holds only in the domain $k\ll 1/d$; in fact, for large d values this expansion is not very meaningful.

In the $d\to\infty$ limit, we observe that $S_{12}(\mathbf{k})\to 0$ and we recover the Debye structure function $S_{11}(\mathbf{k})=\tilde{k}/(1+\tilde{k})$ for the isolated 2D layer. In the more interesting $d=0$ limit where the classical bilayer is collapsed into an isolated 2D layer, the structure functions $S_{11}(\mathbf{k})=(1+\tilde{k})/(2+\tilde{k})$ and $S_{12}(\mathbf{k})=-1/(2+\tilde{k})$ result from Eqs. (9), (6a) and (6b). This is by way of saying that in the $d=0$ limit, there is no longer any distinction between the intralayer and interlayer pair correlation functions $h_{11}(\mathbf{k})$ and $h_{12}(\mathbf{k})$. In this limit, $nh_{11}(\mathbf{k})=nh_{12}(\mathbf{k})=-1/(2+\tilde{k})$, which we can identify as the DH pair correlation function for an isolated layer of density $2n$.

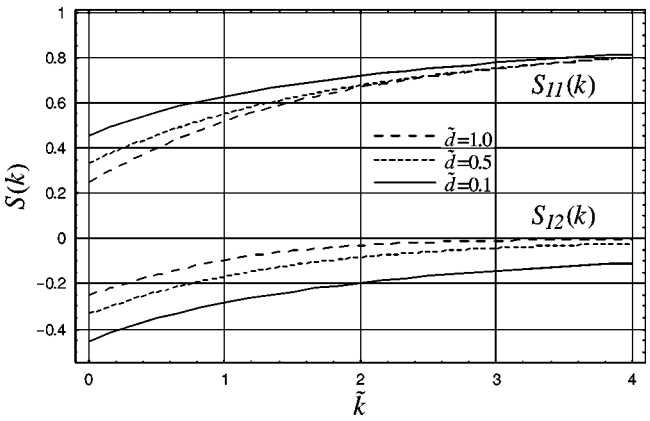

FIG. 1. Bilayer static structure functions $S_{11}(\mathbf{k})$ and $S_{12}(\mathbf{k})$ as functions of dimensionless in-plane wave number $\tilde{k}=k/\kappa$ for layer separations $\tilde{d}=\kappa d=0.1$, 0.5, 1.0; $\kappa=2\pi nZ^2e^2/(k_BT)$ is the 2D Debye wave number.

It is instructive to rotate physical quantities into the space spanned by the $S_+(\mathbf{k})$ in-phase (+) and $S_-(\mathbf{k})$ out-of-phase (−) directions: $S_\pm(\mathbf{k})=S_{11}(\mathbf{k})\pm S_{12}(\mathbf{k})$. One then obtains the compact DH expressions

$$S_\pm(\mathbf{k})=\frac{\tilde{k}}{1+\tilde{k}\pm\exp(-\tilde{k}\tilde{d})}. \tag{11}$$

Then in the long-wavelength limit, one obtains through $O(k^2)$

$$S_+(k\to 0)=\frac{\tilde{k}}{2}-(1-\tilde{d})\frac{\tilde{k}^2}{4}, \tag{12a}$$

$$S_-(k\to 0)=\frac{1}{1+\tilde{d}}+\frac{\tilde{d}^2}{(1+\tilde{d})^2}\frac{\tilde{k}}{2}+\frac{\tilde{d}^3(\tilde{d}-2)\tilde{k}^2}{(1+\tilde{d})^3\ 12}, \tag{12b}$$

in agreement with the RPA limits of the in-phase and out-of-phase compressibility sum rules [15] formulated through $O(\tilde{k}^2)$ and $O(\tilde{k})$, respectively.

C. Pair correlation functions and potentials

The pair correlation functions $h_{ij}(r)$ are calculated from

$$h_{ij}(r)=\gamma\int_0^\infty d\tilde{k}\tilde{k}J_0(\tilde{k}\tilde{r})[S_{ij}(\mathbf{k})-\delta_{ij}]. \tag{13}$$

Figure 1 shows the respective behavior of the $S_{ij}(\mathbf{k})$ struc-

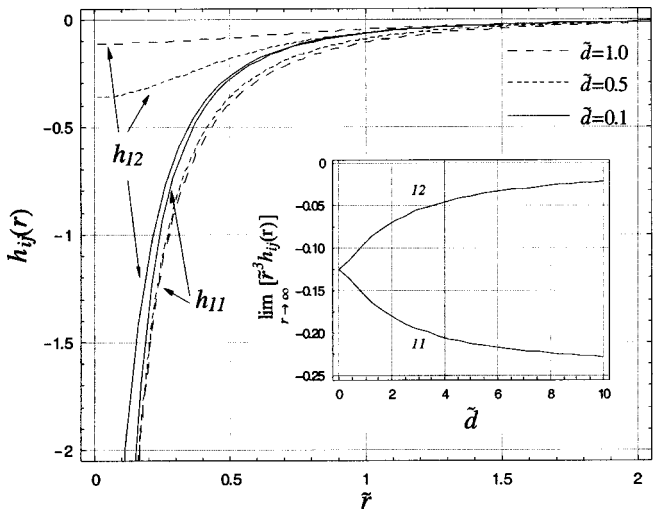

FIG. 2. Bilayer pair correlation functions $h_{11}(\mathbf{r}) = (1/N)\Sigma_{\mathbf{k}}[S_{11}(\mathbf{k})-1]e^{i\mathbf{k}\cdot\mathbf{r}}$ and $h_{12}(\mathbf{r}) = (1/N)\Sigma_{\mathbf{k}} S_{12}(\mathbf{k}) e^{i\mathbf{k}\cdot\mathbf{r}}$ as functions of dimensionless in-plane distance $\tilde{r}=\kappa r$ for layer separations $\tilde{d}=0.1$, 0.5, 1.0 (N is the number of particles per layer). Also shown is the behavior of the screened potentials known to drop off as $1/r^3$ for $r\to\infty$ in the plane of the bilayer. The inset showing $\tilde{r}^3 h_{11}(\mathbf{r})$ and $\tilde{r}^3 h_{12}(\mathbf{r})$ as functions of $\tilde{d}$ for $r\to\infty$ is generated from Eqs. (14a) and (14b).

ture functions, while Fig. 2 shows the behavior of the corresponding $h_{ij}(\mathbf{r})$ pair correlation functions. The divergence of $h_{11}(r\to 0)$ is a well-known defect of the Debye approximation. The relation $h_{ij}(\mathbf{r}) = -1+\exp[-\beta W_{ij}(\mathbf{r})] \approx -\beta W_{ij}(\mathbf{r})$ can be interpreted as defining the potential of the mean field $W_{ij}(\mathbf{r})$. It is the general feature of the Debye approximation that $W_{ij}(\mathbf{r})$ is identical to $\Phi_j^{(i)}(\mathbf{r})$, the screened (total) potential generated in layer j by an impurity of unit charge placed in layer i. Consequently, Fig. 2 also portrays the behavior of

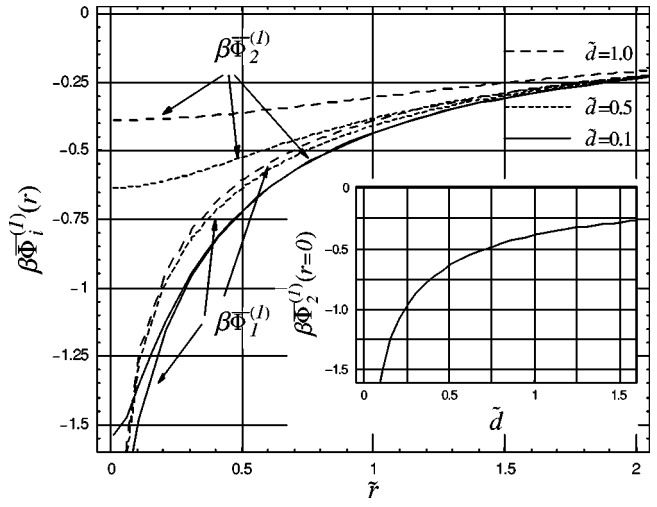

FIG. 3. Bilayer polarization potentials $\bar{\Phi}_1^{(1)}(\mathbf{r})$ and $\bar{\Phi}_2^{(1)}(\mathbf{r})$ as function of dimensionless in-plane distance $\tilde{r}$ for layer separations $\tilde{d}=0.1$, 0.5, 1.0; $\bar{\Phi}_j^{(i)}$ is the polarization potential generated in layer j by an impurity of unit charge placed in layer i. The inset shows the variation of $\bar{\Phi}_2^{(1)}(r=0)$ with $\tilde{d}$.

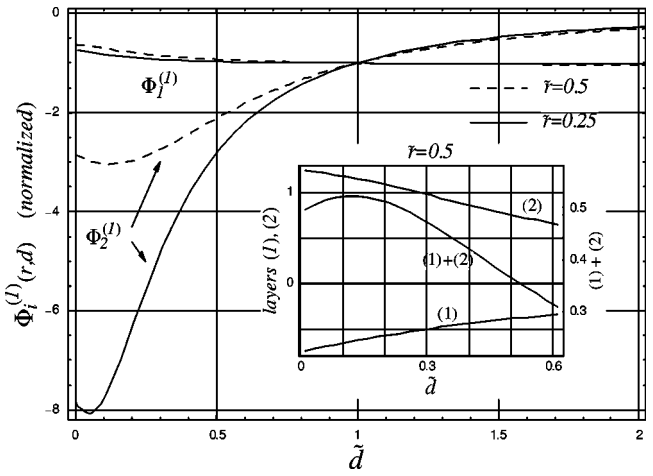

FIG. 4. Bilayer screened potentials $\Phi_1^{(1)}(\mathbf{r},d)$ and $\Phi_2^{(1)}(\mathbf{r},d)$ (normalized with respect to their values at $\tilde{d}=1$) as functions of $\tilde{d}$ for fixed $\tilde{r}=0.25$, 0.5. Note that while $\Phi_1^{(1)}(\mathbf{r},d)$ is a monotonically decreasing function of d, $\Phi_2^{(1)}(\mathbf{r},d)$ is not. The physical explanation is facilitated by the inset showing the variation of the two separate charge contributions to $\Phi_2^{(1)}(\mathbf{r},d)$, one coming from its own layer 2 and the other from layer 1 where the unit charge impurity resides.

the screened potential. Figure 3 shows the behavior of the polarization potential, $\bar{\Phi}_j^{(i)}(\mathbf{r}) = \Phi_j^{(i)}(\mathbf{r}) - \hat{\Phi}_j^{(i)}(\mathbf{r})$; $\hat{\Phi}_j^{(i)}$ is the external potential due solely to the impurity. At the point where the impurity resides, the polarization potential $\bar{\Phi}_1^{(1)}(r=0) = (\beta n/A)\Sigma_{\mathbf{k}}\phi_{1m}(k)\,\eta_{mn}(\mathbf{k})\,\phi_{n1}(k)$ is related to the correlation energy $E_{\rm corr} = \Sigma_i E_{ii} + (1/2)\Sigma_{ij} E_{ij} = 2E_{11} + E_{12}$; $E_{ij} = n^2\Sigma_{\mathbf{k}}\phi_{ij}(k) h_{ij}(\mathbf{k})$ $(i\neq j)$, $E_{ii} = (n^2/2)\Sigma_{\mathbf{k}}\phi_{ii}(k) h_{ii}(\mathbf{k})$. $E_{\rm corr}$ can now be expressed as $E_{\rm corr} = nA\bar{\Phi}_1^{(1)}(r=0)$. Similar to the 2D isolated monolayer in the Debye approximation, the intralayer (11, 22) contributions are logarithmically divergent, whereas the interlayer (12, 21) contributions are finite; the usual remedy for the logarithmic divergence is to invoke the customary κ/γ inverse Landau distance cutoff.

We turn now to the analysis of the d dependence of $\Phi_j^{(i)}(\mathbf{r};d)$ [or equivalently $h_{ij}(\mathbf{r},d)$] at a fixed r. While $\Phi_1^{(1)}(\mathbf{r},d)$ is a monotonically decreasing function of d, $\Phi_2^{(1)}(\mathbf{r},d)$ is not (see Figs. 4 and 5). The physical explanation for this rather counterintuitive behavior can be understood by referring to the inset to Fig. 4 which shows the variation of the two separate charge contributions to $\Phi_2^{(1)}(\mathbf{r},d)$, one coming from charges in its own layer 2 and the other from charges in layer 1 where the impurity resides. The first contribution is negative, because it is generated by the negative screening charge; it decreases in absolute value with increasing d because the amount of total charge in layer 2 decreases with increasing layer separation [cf. Eq. (7b)]. The second contribution is positive because the net charge in layer 1 is positive; it decreases with increasing d because a larger portion of the screening charge accumulates in layer 1 with increasing layer separation [cf. Eq. (7a)]. The combination of these two effects leads to the nonmonotonic behavior as shown in the inset to Fig. 4.

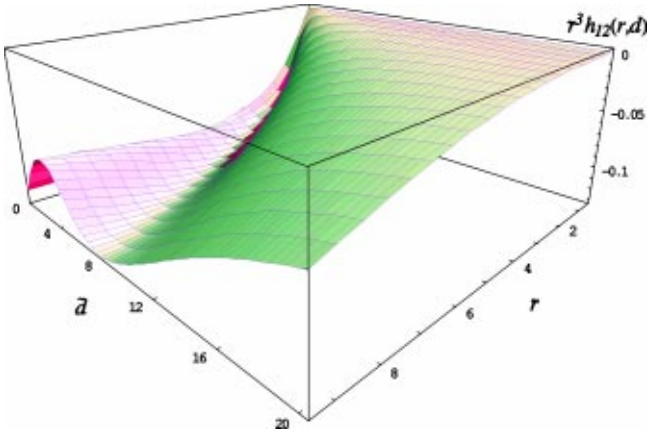

FIG. 5. Bilayer three-dimensional perspective showing variation of $h_{12}(\mathbf{r},d)$ with both $\tilde{r}$ and $\tilde{d}$. Note the strong nonmonotonic variation of $h_{12}(\mathbf{r},d)$ with d for large r values.

D. Asymptotic behavior

It is known that for $r\to\infty$ the screened potential in a 2D layer drops off like $1/r^3$, reflecting the fact that an impurity charge and its screening cloud constitute a quadrupole as the leading contribution to their combined charge distribution. In the bilayer the quadrupole moment is supplemented by a dipole moment in the direction perpendicular to the layers whose potential also drops off as $1/r^3$ for $r\to\infty$ in the plane of the bilayer. The asymptotic expressions resulting from Eq. (13) display this expected behavior (see inset in Fig. 2) with coefficients generated from the $O(k)$ terms in compressibility sum rules (10a) and (10b),

$$\lim_{r\to\infty}\tilde{r}^3 h_{11}(\mathbf{r}) = -\frac{\gamma}{4}\left[1+\left(\frac{\tilde{d}}{1+\tilde{d}}\right)^2\right], \tag{14a}$$

$$\lim_{r\to\infty}\tilde{r}^3 h_{12}(\mathbf{r}) = -\frac{\gamma}{4}\left[1-\left(\frac{\tilde{d}}{1+\tilde{d}}\right)^2\right], \tag{14b}$$

where $\tilde{r}=\kappa r$.

III. SUPERLATTICES

A. Response functions

We turn next to the calculation of the DH structure functions for the infinite superlattice consisting of $N(\to\infty)$ equally spaced electron plasma 2D monolayers, each of large but bounded area A and parallel to the xy plane; d is the spacing between adjacent lattice planes and n is the mean areal density of each monolayer. The periodic structure of the infinite superlattice configuration allows one to introduce direct and inverse Fourier transformations along the z axis, e.g.,

$$\varepsilon(\mathbf{k},q) = \sum_{l=i-j}\varepsilon_{ij}(\mathbf{k})\exp[-iq(z_i-z_j)], \tag{15}$$

$$\varepsilon_{ij}(\mathbf{k}) = \frac{1}{N}\sum_q{}^{*}\ \varepsilon(\mathbf{k},q)\exp[iq(z_i-z_j)], \tag{16}$$

where $z_j=jd$ $(j=0,\pm1,\pm2,...)$ locates the jth layer above or below the reference lattice plane at $z=0$. The Σ^* notation indicates that the summation is restricted to the first Brillouin zone. We observe that for the infinite superlattice, quantities such as $\varepsilon_{ij}(k)$, $S_{ij}(k)$, etc. remain invariant under translation of their layer indices, e.g., $\varepsilon_{ij}=\varepsilon_{i-j,0}$.

Proceeding as in Sec. II, we introduce the interaction potential

$$\phi(k,q) = \frac{2\pi e^2}{k}F(k,q), \tag{17}$$

where the well-known superlattice form factor

$$F(k,q) = \frac{\sinh kd}{\cosh kd-\cos qd} \tag{18}$$

is the layer-space Fourier transform [prescribed by Eq. (15)] of $\exp(-k|z_i-z_j|)$. The superlattice counterparts of Eqs. (1), (2), and (3) are then given by

$$\varepsilon(\mathbf{k},q) = 1-\phi(k,q)\overline{\chi}(\mathbf{k},q), \tag{19}$$

$$\chi(\mathbf{k},q) = \overline{\chi}(\mathbf{k},q)\,\eta(\mathbf{k},q), \tag{20}$$

$$\eta(\mathbf{k},q) = 1+\phi(k,q)\chi(\mathbf{k},q); \tag{21}$$

$\overline{\chi}(\mathbf{k},q)$ and $\chi(\mathbf{k},q)$ are the screened (total) and full (external) density response functions, respectively, and $\eta(\mathbf{k},q)=1/\varepsilon(\mathbf{k},q)$ is the inverse dielectric response function.

Paralleling the weak coupling calculation of Sec. II, Eqs. (20), (21), and the density response of the noninteracting gas,

$$\overline{\chi}(\mathbf{k},q) = -\beta n, \tag{22}$$

yield the full density response and inverse dielectric functions

$$\chi(\mathbf{k},q) = -\beta n\,\eta(\mathbf{k},q), \tag{23}$$

$$\eta(\mathbf{k},q) = \frac{1}{1+\dfrac{1}{\tilde{k}}F(k,q)}. \tag{24}$$

The zero-temperature degenerate RPA equivalent of Eq. (23) has been calculated in Ref. [12].

B. Structure functions

Invoking the superlattice static FDT [19],

$$S(\mathbf{k},q) = -\frac{1}{\beta n}\chi(\mathbf{k},q), \tag{25}$$

and the RPA full density response (23), one readily obtains

$$S(\mathbf{k},q) = \eta(\mathbf{k},q). \tag{26}$$

At long wavelengths the structure function assumes the form

$$S(k\to 0,q)=\frac{1-\cos qd}{1-\cos qd+\tilde{d}}+\frac{2+\cos qd}{(1-\cos qd+\tilde{d})^2}\frac{\tilde{d}^3\tilde{k}^2}{6}, \tag{27}$$

consistent with the out-of-phase compressibility rule

$$S(k\to 0,q)=\frac{1-\cos qd}{L(q)(1-\cos qd)+\tilde{d}} + \frac{2+\cos qd}{[L(q)(1-\cos qd)+\tilde{d}]^2}\frac{\tilde{d}^3\tilde{k}^2}{6}; \tag{28}$$

$$L(q)\equiv\beta\sum_{l=i-j}\left(\frac{\partial P_i}{\partial n_j}\right)_T\exp[-iq(z_i-z_j)] \tag{29}$$

is the inverse compressibility function that in the RPA limit is equal to unity for all values of q. In the $q=0$ (in-phase) limit, the system exhibits 3D one-component-plasma (OCP)-like behavior portrayed by the long-wavelength expansion of the structure function,

$$S(k\to 0,q=0)=\frac{k^2}{\kappa_{3D}^2}-\frac{k^4}{\kappa_{3D}^4}\left[1+\frac{\kappa_{3D}^2d^2}{12}\right], \tag{30}$$

consistent with the in-phase compressibility sum rule [16]; $\kappa_{3D}=\sqrt{4\pi ne^2\beta/d}$ is the 3D-like Debye wave number for the superlattice.

In order to see the behavior of the individual lattice planes, one can generate the hierarchy of structure functions $S_{0m}(\mathbf{k})$, $(m=0,\pm 1,\pm 2,...)$ from Eqs. (24), (26), and

$$S_{0m}(\mathbf{k})=\frac{1}{N}\sum_q{}^{*}\,S(\mathbf{k},q)\exp(iqmd) =\frac{d}{2\pi}\int_{-\pi/d}^{\pi/d}dqS(\mathbf{k},q)\exp(iqmd). \tag{31}$$

Carrying out the integration, one obtains

$$S_{0m}(\mathbf{k})=\delta_{0m}-\frac{\left[K(\tilde{k},\tilde{d})-\sqrt{K^2(\tilde{k},\tilde{d})-1}\right]^{|m|}}{\sqrt{K^2(\tilde{k},\tilde{d})-1}}\frac{\sinh\tilde{k}\tilde{d}}{\tilde{k}}, \quad (m=0,\pm 1,\pm 2,...) \tag{32}$$

$$K(\tilde{k},\tilde{d})\equiv\frac{\sinh\tilde{k}\tilde{d}}{\tilde{k}}+\cosh\tilde{k}\tilde{d}. \tag{33}$$

It is of some interest to display the intralayer $m=0$ and nearest neighbor $m=1$ Debye structure functions individually [14,19b]

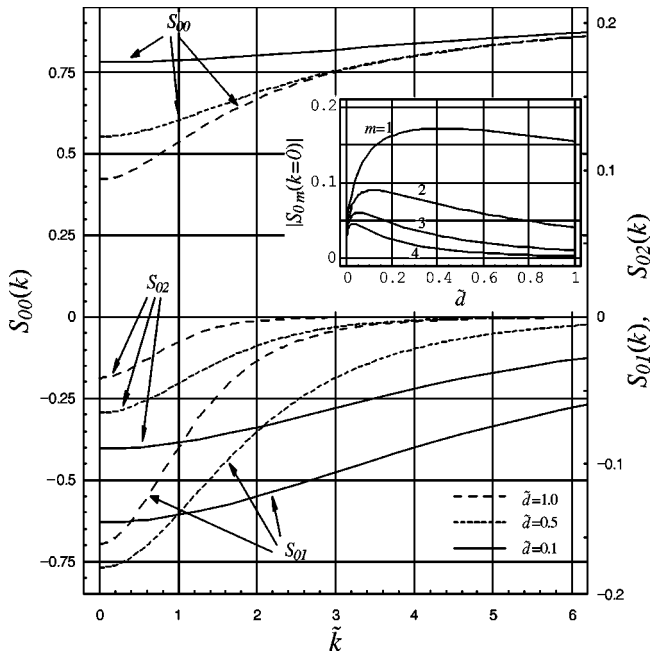

FIG. 6. Superlattice static structure functions $S_{00}(\mathbf{k})$, $S_{01}(\mathbf{k})$, and $S_{02}(\mathbf{k})$ as functions of dimensionless in-plane wave number $\tilde{k}$ for layer separations $\tilde{d}=0.1$, 0.5, 1.0. The inset, generated from Eq. (36), shows the nonmonotonic variation of $|S_{0m}(k=0)|$ with $\tilde{d}$ for layer indices $m=1,2,3,4$. Note that $S_{0m}(k=0)$ also represents the total charge residing in lattice plane $m\neq 0$.

$$S_{00}(\mathbf{k})=1-\frac{1}{\sqrt{1+\tilde{k}^2+2\tilde{k}\coth\tilde{k}\tilde{d}}}, \tag{34}$$

$$S_{01}(\mathbf{k})=\frac{1}{\tilde{k}}\sinh\tilde{k}\tilde{d}\left\{1-\frac{1+\tilde{k}\coth\tilde{k}\tilde{d}}{\sqrt{1+\tilde{k}^2+2\tilde{k}\coth\tilde{k}\tilde{d}}}\right\}. \tag{35}$$

Figure 6 shows the variation of the structure functions $S_{00}(\mathbf{k})$, $S_{01}(\mathbf{k})$, and $S_{02}(\mathbf{k})$ with $\tilde{k}$.

At long wavelengths the small-k expansion of Eq. (32) yields

$$S_{0m}(k\to 0)\approx\delta_{0m}-\sqrt{\frac{\tilde{d}}{2+\tilde{d}}}\left[(1+\tilde{d})-\sqrt{\tilde{d}(2+\tilde{d})}\right]^{|m|} \times\left\{1-\frac{\tilde{d}^2}{6}\left[\frac{3+2\tilde{d}}{\tilde{d}(2+\tilde{d})}+\frac{|m|(3+\tilde{d})}{\sqrt{\tilde{d}(2+\tilde{d})}}\right]\tilde{k}^2\right\}. \tag{36}$$

We note that the matrix elements $\eta_{00}(k=0)-1=-\sqrt{\tilde{d}/(2+\tilde{d})}$ and $\eta_{0m}(k=0)$ $(m=\pm 1,\pm 2,\pm 3,...)$ given directly by $S_{0m}=\eta_{0m}$ from Eq. (36) represent the total screening charges residing in lattice plane 0 and in all the other $(m\neq 0)$ lattice planes, respectively, surrounding a $Z=\pm 1$ impurity charge in lattice plane 0. It is remarkable that, in contrast to the expected monotonic decrease of the screening

charge in the mth ($m\neq 0$) lattice plane with increasing d [cf. Eq. (7) for the bilayer], the charge exhibits a maximum at some $d=d_m$ value (see inset in Fig. 6). The physical explanation for this behavior is discussed below.

The nonanalytic behavior in $\tilde{d}$ exhibited in Eq. (36) is quite remarkable, especially so when compared with Eqs. (10a) and (10b) for small k and the combination of Eqs. (9), (6), and (7) for arbitrary k. This feature notwithstanding, the total $S(\mathbf{k},q=0)$ reverts to its expected analytic behavior,

$$
\begin{aligned}
S(\mathbf{k},q=0) &= \sum_{m=-\infty}^{\infty} S_{0m}(\mathbf{k}) \\
&= 1-\frac{\sinh\tilde{k}\tilde{d}}{\tilde{k}\sqrt{K^2-1}}\sum_{m=-\infty}^{\infty}[K-\sqrt{K^2-1}]^{|m|} \\
&= 1+\frac{\sinh\tilde{k}\tilde{d}}{\tilde{k}\sqrt{K^2-1}}\left\{1-2\sum_{m=0}^{\infty}[K-\sqrt{K^2-1}]^{|m|}\right\} \\
&= 1+\frac{\sinh\tilde{k}\tilde{d}}{\tilde{k}\sqrt{K^2-1}}-\frac{2\sinh\tilde{k}\tilde{d}}{\tilde{k}\sqrt{K^2-1}}\left[\frac{1}{1-K+\sqrt{K^2-1}}\right] \\
&= 1-\frac{\sinh\tilde{k}\tilde{d}}{\tilde{k}(K-1)} = \frac{1}{1+\dfrac{F(k,0)}{\tilde{k}}}. \qquad (37)
\end{aligned}
$$

C. Correlation functions and potentials

We turn now to the equilibrium pair correlation functions $h_{00}(r)$, $h_{01}(r)$, and $h_{02}(r)$, which are generated from

$$
h_{0m}(\mathbf{r})=\gamma\int_0^{\infty}d\tilde{k}\tilde{k}J_0(\tilde{k}\tilde{r})[S_{0m}(\mathbf{k})-\delta_{0m}], \qquad (38)
$$

and displayed in Fig. 7. The divergence of $h_{00}(r\to 0)$ is again a well-known defect of the Debye approximation.

The development of the relationships among the superlattice pair correlation functions, the potentials, and the correlation energy follows the same pattern as in the bilayer case. Similarly to the bilayer, the relation $h_{0m}(\mathbf{r})=-1+\exp[-\beta W_{0m}(\mathbf{r})]\approx-\beta W_{0m}(\mathbf{r})$ can be interpreted as defining the potential of the mean field $W_{0m}(\mathbf{r})$; in the Debye approximation, $W_{0m}(\mathbf{r})$ is identical to $\Phi_m^{(0)}(\mathbf{r})$, the screened (total) potential generated in lattice plane m by an impurity of unit charge placed in reference plane 0. Consequently, Fig. 7 also portrays the behavior of the screened potential. Figure 8 shows the behavior of the polarization potential, $\bar{\Phi}_m^{(0)}(\mathbf{r})=\Phi_m^{(0)}(\mathbf{r})-\hat{\Phi}_m^{(0)}(\mathbf{r})$; $\hat{\Phi}_m^{(0)}$ is the external potential due solely to the impurity. To see how the polarization potential relates to the correlation energy, we first observe that for an N-layer structure with the 0-lattice plane located at the bottom of the stack, the correlation energy is $E_{corr}=NE_{00}+\Sigma_{m=1}^{N-1}(N-m)E_{0m}$; $E_{0m}=n^2\Sigma_{\mathbf{k}}\phi_{0m}(k)h_{0m}(\mathbf{k})(m\neq 0)$, $E_{00}=(n^2/2)\Sigma_{\mathbf{k}}\phi_{00}(k)h_{00}(\mathbf{k})$. For the case of the infinite superlattice (with the 0 lattice plane relocated to the interior of the stack), the correlation energy is therefore given by $E_{corr}=\Sigma_i E_{ii}+(1/2)\Sigma_{i\neq j}E_{ij}=NE_{00}+(N/2)\Sigma_{m=1}^{\infty}E_{0m}$. Then the polarization potential at the point where the particle resides, $\bar{\Phi}_0^{(0)}(r=0)=(\beta n/A)\Sigma_{\mathbf{k}}\phi_{0m}(k)\,\eta_{mn}(\mathbf{k})\,\phi_{n0}(k)$, is related to the correlation energy through $E_{corr}=(N/2)nA\bar{\Phi}_0^{(0)}(r=0)$. Similarly to the bilayer and the 2D monolayer, the intralayer E_{00} contribution is logarithmically divergent, whereas the interlayer E_{0m} ($m=1,2,...$) contributions are finite. The polar-

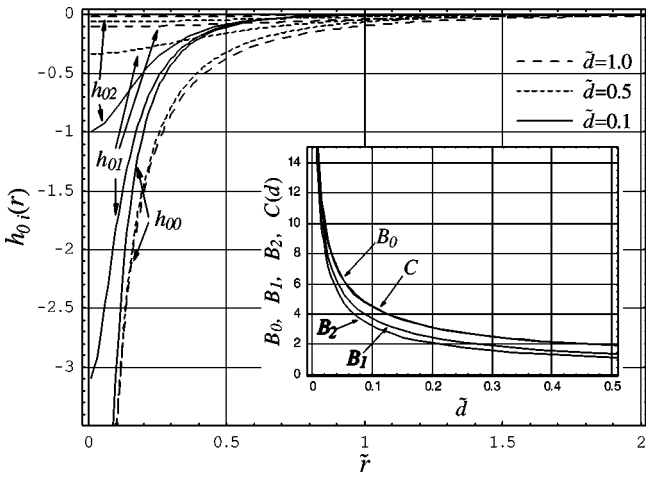

FIG. 7. Superlattice pair correlation functions $h_{00}(\mathbf{r})$, $h_{01}(\mathbf{r})$, and $h_{02}(\mathbf{r})$ as functions of dimensionless in-plane distance $\tilde{r}$ for layer separations $\tilde{d}=0.1$, 0.5, 1.0. It also portrays the behavior of the screened potentials $\Phi_0^{(0)}(\mathbf{r})$, $\Phi_1^{(0)}(\mathbf{r})$, and $\Phi_2^{(0)}(\mathbf{r})$; $\Phi_m^{(0)}(\mathbf{r})$ is the (total) screened potential generated in layer m by an impurity of unit charge placed in reference layer 0. The inset shows the variation of the exponential decay constants $B_0(\tilde{d})$, $B_1(\tilde{d})$, and $B_2(\tilde{d})$ calculated from Eq. (42). The exponential decay constant $C(\tilde{d})$ [which very nearly coincides with $B_0(\tilde{d})$] refers to the asymptotic ($m\to\infty$) behavior of $h_{0m}(r=0)$ along the z axis.

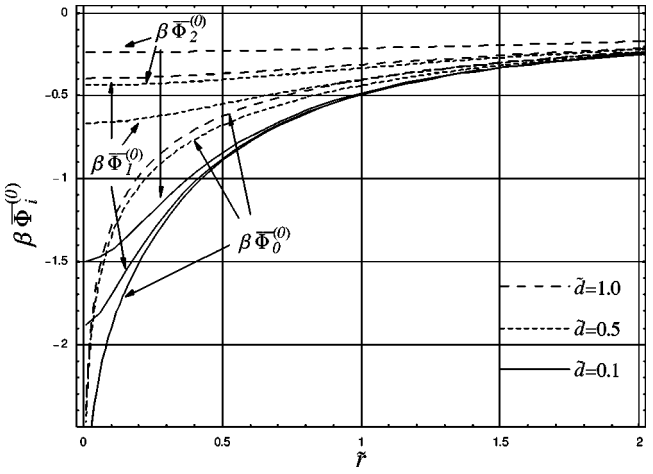

FIG. 8. Superlattice polarization potentials $\bar{\Phi}_0^{(0)}(\mathbf{r})$, $\bar{\Phi}_1^{(0)}(\mathbf{r})$, and $\bar{\Phi}_2^{(0)}(\mathbf{r})$ as functions of in-plane dimensionless distance $\tilde{r}$ for separation distance $\tilde{d}=0.1$, 0.5, 1.0.

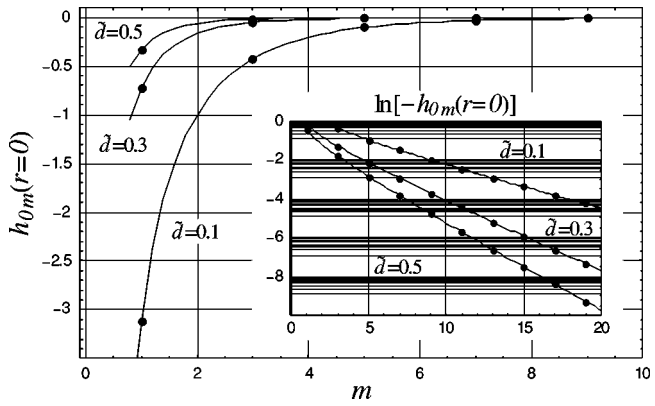

FIG. 9. Superlattice pair correlation function $h_{0m}(r=0)$ as a function of layer index m for $\tilde{d}=0.1$, 0.3, 0.5. The inset indicates that as $m\to\infty$, a 3D-like behavior similar to Eq. (39) prevails along the superlattice axis.

ization potentials $\overline{\Phi}_m^{(0)}(r=0)$ $(m=\pm1,\pm2,...)$ in the adjacent lattice planes also remain finite. Unlike the bilayer, however, in the $d\to0$ limit, the system assumes a 3D-like behavior marked by the disappearance of the logarithmic divergence with $\overline{\Phi}_0^{(0)}(r\to0)\approx e^2\kappa_{3D}$.

D. Asymptotic behavior

In contrast to the bilayer configuration, the large-r behavior of the screened potentials is not given by an inverse power law, since for $r\to\infty$ the superlattice behaves like a 3D bulk system. Indeed, for d sufficiently small $(\tilde{d}\to0)$, the asymptotic behavior of the $|m|=0,1,2,3,...$ hierarchy of screened potentials can be well described by the 3D OCP-like formula

$$h_{0m}(r\to\infty)=-\beta\Phi_m^{(0)}(r\to\infty)\approx A_m(1/\tilde{r})\exp(-B_m\tilde{r}) \tag{39}$$

fitted to $h_{0m}(\mathbf{r})$ computed from Eqs. (38) and (32). Analytical formulas for $A_m(\tilde{d})$ and $B_m(\tilde{d})$ can be derived by equating the small-k Debye structure function (36) to the small-k equivalent of Eq. (39),

$$S_{0m}(k\to0)\approx\delta_{0m}+\frac{A_m(\tilde{d})}{\gamma B_m(\tilde{d})}\left[1-\frac{\tilde{k}^2}{2B_m^2(\tilde{d})}\right]. \tag{40}$$

One obtains

$$A_m(\tilde{d})=-\frac{\gamma\sqrt{3}\left[(1+\tilde{d})-\sqrt{\tilde{d}(2+\tilde{d})}\right]^{|m|}}{(3+2\tilde{d})+|m|(3+\tilde{d})\sqrt{\tilde{d}(2+\tilde{d})}}<0, \tag{41}$$

$$B_m(\tilde{d})=\sqrt{3}\sqrt{\frac{1+(2/\tilde{d})}{3+2\tilde{d}+|m|(3+\tilde{d})\sqrt{\tilde{d}(2+\tilde{d})}}}. \tag{42}$$

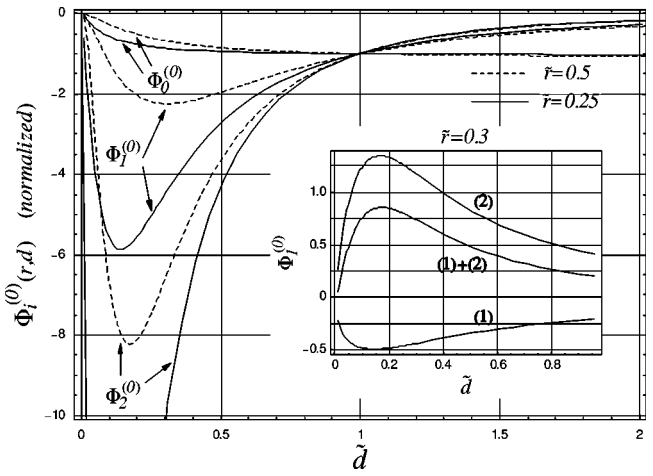

FIG. 10. Superlattice screened potentials $\Phi_0^{(0)}(\mathbf{r},d)$, $\Phi_1^{(0)}(\mathbf{r},d)$, and $\Phi_2^{(0)}(\mathbf{r},d)$ (normalized with respect to their values at $\tilde{d}=1$) as functions of $\tilde{d}$ for fixed $\tilde{r}=0.25$, 0.5. Note the nonmonotonic d dependence similar to that found in the bilayer configuration: the physical explanation is facilitated by the inset showing the variation of the two separate charge contributions to $\Phi_1^{(0)}(\mathbf{r},d)$, one coming from its own layer 1, where the potential is measured, and the other from reference layer 0, where the unit charge impurity resides.

The above analytical expressions for $B_0(\tilde{d})$, $B_1(\tilde{d})$, and $B_2(\tilde{d})$ are displayed in the inset to Fig. 7.

Comparison of $S_{01}(\mathbf{k})$ and $S_{02}(\mathbf{k})$ shows the expected decay of correlations with increasing m. To analyze this point further, we have calculated $h_{0m}(r=0)$. Its behavior as a function of the layer index m is displayed in Fig. 9. As $m\to\infty$, one would expect that a 3D behavior similar to Eq. (39) prevails in the z direction. This is corroborated by the inset to Fig. 9 which also shows that as $d\to0$, $h_{0m}(r=0)$ becomes proportional to $(1/|m|d)\exp(-|m|\kappa_{3D}d)$. The comparison of the decay constants along the z axis and in-plane directions is shown in the inset in Fig. 7. There is no discernable difference between the decay constants B_m and C pertaining to the r and z directions, respectively, that would indicate an anisotropy of the screening. A similar conclusion was reached by Visscher and Falicov [12].

E. *d* dependence

As to the d dependence of the $\Phi_m^{(0)}(\mathbf{r},d)$, or equivalently of the $h_{0m}(\mathbf{r},d)$, at a fixed r, one encounters a nonmonotonic d dependence similar to that found in the bilayer configuration (Figs. 10 and 11). Unlike the bilayer, however, the superlattice exhibits more pronounced extrema and the physical mechanism leading to the development of the extrema is somewhat different. The difference originates from the peculiar $d\to0$ behavior of the superlattice. In this limit, all the lattice planes (an infinite number of them) share the screening charge equally and therefore, in contrast to the bilayer, the screening charge on each individual lattice plane goes to zero. As the lattice planes recede from each other, the nearest layers assume their privileged role by acquiring the biggest share of the screening charge. Thus the screening charge in

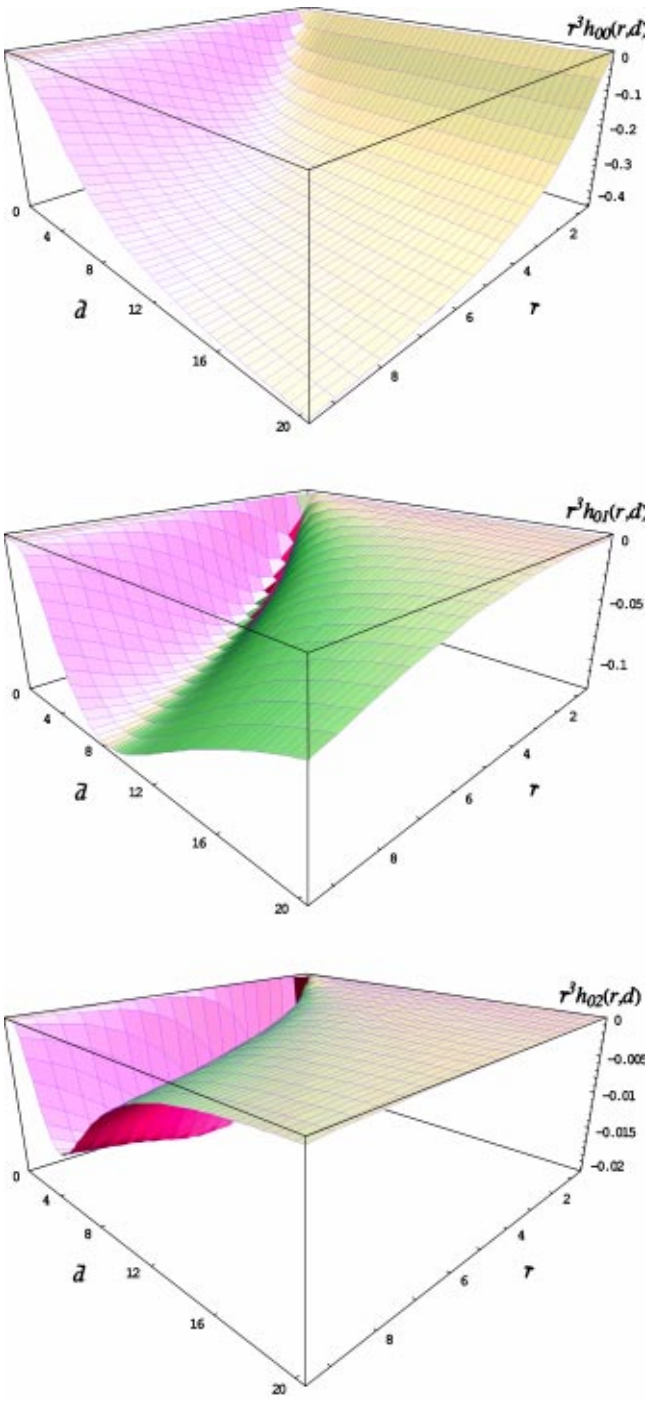

FIG. 11. Superlattice three-dimensional perspective showing variation of $h_{00}(\mathbf{r},d)$, $h_{01}(\mathbf{r},d)$, and $h_{02}(\mathbf{r},d)$ with both $\tilde{r}$ and $\tilde{d}$. Note the difference in the behavior of h as a function of d between the bilayer (Fig. 5) and the superlattice (this figure).

these lattice planes increases to a maximum at some critical separation d_m, as can be inferred from the discussion immediately following Eq. (36). Further increase of d, however, leads to a decrease of the screening charge for reasons discussed in relation to the bilayer. This behavior is shown in the inset to Fig. 10. The extrema in $\Phi_m^{(0)}(\mathbf{r},d)$ are now the combined result of the nonmonotonic variation of the screening charge (peculiar to the infinite superlattice) and of the effect shared with the bilayer as described in Sec. II (see inset to Fig. 4).

Finally, we note a remarkable recursion relation that makes it possible to generate the hierarchy of Fourier-transformed interlayer pair correlation functions $h_{0m}(\mathbf{k})$ $(m\neq 0)$ from $h_{01}(\mathbf{k})$ and $h_{00}(\mathbf{k})$. From Eq. (32) and the relation $S_{0m}(\mathbf{k})=\delta_{0m}+nh_{0m}(\mathbf{k})$, we observe that

$$h_{0m}(\mathbf{k})=[h_{00}(\mathbf{k})]^{1-|m|}[h_{01}(\mathbf{k})]^{|m|}. \tag{43}$$

A more illuminating way of expressing the same relationship is by way of introducing the transfer function $t(\mathbf{k})$ $=h_{01}(\mathbf{k})/h_{00}(\mathbf{k})=K-\sqrt{K^2-1}$; Eq. (43) then becomes

$$h_{0m}(\mathbf{k})=[t(\mathbf{k})]^{|m|}h_{00}(\mathbf{k}). \tag{44}$$

In view of Eq. (26), similar recursion relations exist for $\eta_{0m}(\mathbf{k})$. The existence of the latter was postulated, but not derived, by Visscher and Falicov [12].

IV. CONCLUSIONS

In this paper we have developed an equivalent of the Debye-Hückel (DH) weakly coupled equilibrium theory for layered classical charged particle systems composed of one single charged species. We have considered the two most important configurations, the charged particle bilayer and the infinite superlattice. The approach is based on the link provided by the classical fluctuation-dissipation theorem between the RPA response functions and the Debye equilibrium pair correlation function [bilayer Eq. (8) and superlattice Eq. (25)]. The DH results are of fundamental interest since they are based on the only exact calculation available for layered systems and, as such, elucidate the effect of the interlayer separation on particle correlations.

We have calculated pair correlation functions $h_{ij}(\mathbf{r})$, screened and polarization potentials $\Phi_j^{(i)}(\mathbf{r})$ and $\overline{\Phi}_j^{(i)}(\mathbf{r})$, static structure functions $S_{ij}(\mathbf{k})$, and static response functions $\chi_{ij}(\mathbf{k})$, $\eta_{ij}(\mathbf{k})$ in layer space, and in addition, in the case of the superlattice, in the Fourier $(\mathbf{k}, q)$ representation. The values of the latter in the $k\rightarrow 0$ limit are consistent with the earlier derived [9,15–17] perfect screening and compressibility sum rules. With the aid of the sum rules one can analyze the asymptotic behavior of the correlation functions and verify the expected algebraic r^{-3} decay (for the bilayer) and exponential decay (for the superlattice) for $r\rightarrow\infty$. The monotonic decay of $h_{ij}(\mathbf{r})$ in r [or of $S_{ij}(\mathbf{k})$ in k], characteristic of the weakly correlated regime, prevails for all layer separations. On the other hand, the rather unexpected behavior that emerges from the analysis is the marked nonmonotonic dependence of the screened potential and of the correlations on the layer separation d. In other words, in a certain parameter domain an increase in the distance between layers leads to a locally enhanced screened potential or correlation. In the case of the superlattice, for small d values, the

quasi-3D character of the system renders a different physical reason for a similar nonmonotonic behavior even of the total screening charges carried by the individual lattice planes. It would be interesting to contemplate the possible experimental verification of these effects.

ACKNOWLEDGMENTS

This work was supported by Grant Nos. DE-FG02-98ER54491 (K.I.G.) and DE-FG02-98ER54501 (G.J.K. and S.K.) and INT-0002200 (G.J.K.).

[1] (a) M. G. Raizen, J. M. Gilligan, J. C. Bergquist, W. M. Itano, and D. J. Wineland, Phys. Rev. A **45**, 6493 (1992); (b) J. J. Bollinger, D. J. Wineland, and D. H. E. Dubin, Phys. Plasmas **1**, 1403 (1994); (c) J. N. Tan, J. J. Bollinger, B. M. Jelenković, W. M. Itano, and D. J. Wineland, in *Physics of Strongly Coupled Plasmas*, edited by W. D. Kraeft and M. Schlanges (World Scientific, Singapore, 1996), p. 387; (d) T. B. Mitchell, J. J. Bollinger, D. H. E. Dubin, X.-P. Huang, W. M. Itano, and R. H. Bundham, Science **282**, 1290 (1998).

[2] (a) D. H. E. Dubin, Phys. Rev. Lett. **66**, 2076 (1991); (b) **71**, 2753 (1993); Phys. Fluids B **5**, 295 (1993).

[3] (a) V. A. Schweigert, I. V. Schweigert, A. Melzer, A. Homann, and A. Piel, Phys. Rev. E **64**, 4155 (1996); (b) Y. Hayashi and K. Ṭachibana, Jpn. J. Appl. Phys., Part 2 **33**, L804 (1994).

[4] L. Świerkowski, D. Neilson, and J. Szymański, Phys. Rev. Lett. **67**, 240 (1991).

[5] F. Rapisada and G. Senatore, in *Strongly Coupled Coulomb Systems*, edited by G. Kalman, K. Blagoev, and M. Rommel (Plenum Press, New York, 1998), p. 529.

[6] (a) G. Goldoni and F. M. Peeters, Phys. Rev. B **53**, 4591 (1996); (b) in *Proceedings of the 23rd International Conference on the Physics of Semiconductor Physics*, edited by M. Scheffer and R. Zimmermann (World Scientific, Singapore, 1996), Vol. 3; (c) Europhys. Lett. **33**, 293 (1997).

[7] V. I. Falko, Phys. Rev. B **49**, 7774 (1994).

[8] V. Valtchinov, G. Kalman, and K. B. Blagoev, Phys. Rev. E **56**, 4351 (1997).

[9] G. J. Kalman, K. B. Blagoev, Z. Donko, K. I. Golden, G. McMullan, V. Valtchinov, and H. Zhao, J. Phys. (Paris), Colloq. **10**, 585 (2000).

[10] (a) Z. Donko and G. J. Kalman, Phys. Rev. E **63**, 061504 (2001); (b) J. Phys. (Paris), Colloq. **10**, 5355 (2000).

[11] J.-J. Weis, D. Levesque and S. Jorge, Phys. Rev. B **63**, 045308 (2001).

[12] P. B. Visscher and L. M. Falicov, Phys. Rev. B **3**, 2541 (1971).

[13] G. Kalman, Y. Ren, and K. I. Golden, Phys. Rev. B **50**, 2031 (1994); Dexin Lu, K. I. Golden, G. Kalman, P. Wyns, L. Miao, and X.-L. Shi, *ibid.* **54**, 11 457 (1996).

[14] G. Kalman, Y. Ren, and K. I. Golden, Contrib. Plasma Phys. **33**, 449 (1993).

[15] G. J. Kalman and K. I. Golden (unpublished).

[16] G. J. Kalman, Z. Donko, K. I. Golden, and G. McMullan, *Charged Particle Bilayers: Structure and Dynamics*, Condensed Matter Theories 16 (Nova Science New York, 2001), pp. 51–59.

[17] G. J. Kalman, Z. Donko, and K. I. Golden, Contrib. Plasma Phys. **41**, 191 (2001).

[18] G. Kalman and K. I. Golden, Phys. Rev. A **29**, 844 (1984).

[19] (a) K. I. Golden and De-xin Lu, Phys. Rev. A **45**, 1084 (1992); (b) G. Kalman and K. I. Golden, in *Condensed Matter Theories*, edited by L. Blum and F. B. Malik (Plenum Press, New York, 1993) Vol. 8, pp. 127–137; (c) K. I. Golden, in *Modern Perspectives in Many-Body Physics*, edited by M. P. Das and J. Mahanty (World Scientific, Singapore, 1994), pp. 315–346.